

กำเนิดเชิงศิวาวิทยาของหินแปลกปลอมอุ้มพลอยทับทิม  
จากศิลาภูมิประเทศหินบะซอลต์ บริเวณเมืองซิมบาและเมืองอิมาลี ประเทศเคนยา



นายรัชชัย เชื้อเหล่าวานิช

วิทยานิพนธ์นี้เป็นส่วนหนึ่งของการศึกษาตามหลักสูตรปริญญาวิทยาศาสตรดุษฎีบัณฑิต

สาขาวิชาธรณีวิทยา ภาควิชาธรณีวิทยา

คณะวิทยาศาสตร์ จุฬาลงกรณ์มหาวิทยาลัย

ปีการศึกษา 2553

ลิขสิทธิ์ของจุฬาลงกรณ์มหาวิทยาลัย



**PETROGENESIS OF RUBY-BEARING XENOLITH  
FROM SIMBA AND EMALI BASALTIC TERRANES, KENYA**

**Mr. Tawatchai Chualaowanich**

**A Dissertation Submitted in Partial Fulfillment of the Requirements  
for the Degree of Doctor of Philosophy Program in Geology**

**Department of Geology**

**Faculty of Science**

**Chulalongkorn University**

**Academic Year 2010**


**Copyright of Chulalongkorn University**

**531928**

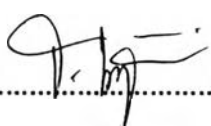
Thesis Title                    PETROGENESIS OF RUBY-BEARING XENOLITH  
FROM SIMBA AND EMALI BASALTIC TERRANES, KENYA  
By                                    Mr. Tawatchai Chualaowanich  
Field of Study                 Geology  
Thesis Advisor                Assistant Professor Chakkaphan Sutthirat, Ph.D.  
Thesis Co-advisor           Associate Professor Visut Pisuttha-Arnond, Ph.D.

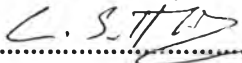
---

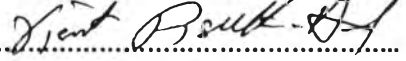
Accepted by the Faculty of Science, Chulalongkorn University in Partial  
Fulfillment of the Requirements for the Doctoral Degree


  
..... Dean of the Faculty of Science  
(Professor Supot Hannongbua, Dr.rer.nat.)


THESIS COMMITTEE

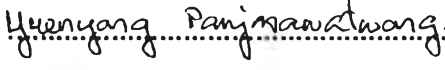
  
..... Chairman  
(Thanop Thitimakorn, Ph.D.)


  
..... Thesis Advisor  
(Assistant Professor Chakkaphan Sutthirat, Ph.D.)

  
..... Thesis Co-advisor  
(Associate Professor Visut Pisuttha-Arnond, Ph.D.)

  
..... Examiner  
(Assistant Professor Somchai Nakapadungrat, Ph.D.)

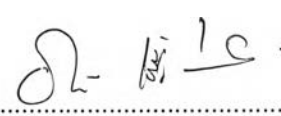
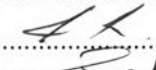
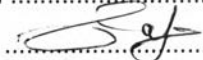
  
..... Examiner  
(Vichai Chutakasitkanon, Ph.D.)

  
..... External Examiner  
(Associate Professor Yuenyong Panjasawatwong, Ph.D.)

  
..... External Examiner  
(Prinya Putthapiban, Ph.D.)

รวิชัย เชื้อเหล้าวานิช: กำเนิดเชิงศิลาวิทยาของหินแปรกล่อมอุ้มพลอยทับทิมจากศิลา  
ภูมิประเทศหินบะซอลต์ บริเวณเมืองซิมบาและเมืองอิมาลี ประเทศเคนยา  
(PETROGENESIS OF RUBY-BEARING XENOLITH FROM SIMBA AND EMALI  
BASALTIC TERRANES, KENYA) อ. ที่ปริกษานิพนธ์หลัก: ผศ.ดร. จักรพันธ์  
สุทธิรัตน์, อ. ที่ปริกษานิพนธ์ร่วม: รศ.ดร. วิสุทธิ พิสุทธิอรานนท์, 110 หน้า.

งานวิจัยนี้มุ่งเน้นศึกษาการกำเนิดเชิงศิลาวิทยาของหินแปรกล่อมอุ้มพลอยทับทิมที่พบ  
มากในพื้นที่ศิลาภูมิประเทศหินบะซอลต์ขนาดเล็ก 2 บริเวณ คือ บริเวณกลุ่มเนินภูเขาไฟเซาญู และ  
บริเวณกลุ่มเนินภูเขาไฟกัลย ไกลกับเมืองซิมบา ในภูมิภาคตะวันออกเฉียงใต้ของประเทศเคนยา ซึ่งศิลา  
ภูมิประเทศทั้งสองนี้จัดเป็นส่วนหนึ่งของเขตหินภูเขาไฟไซลูลูตอนเหนือ พบว่าหินบะซอลต์บริเวณ  
นี้เป็นเนื้ออัลคาไลที่มีองค์ประกอบอยู่ในช่วง ฟอยไดต์ ถึง เทไฟรต์/บาซาไนต์ โดยมีลักษณะ  
องค์ประกอบทางเคมีที่บ่งชี้ถึงแหล่งต้นกำเนิดแมกมาที่มีแร่แอมฟิโบลและ/หรือฟลโกไปต์เป็น  
ส่วนประกอบที่ผ่านการหลอมละลายบางส่วน จากผลของกระบวนการร่วมสัมพันธ์ระหว่าง  
mantle plume กับโครงสร้างที่ได้จากการคลายแรงที่เกิดขึ้นจากการชนกันของแผ่นเปลือกโลกที่  
ก่อเกิดแนวเทือกเขาโมซัมบิกในอดีต (~600-800 ล้านปี) ทั้งนี้บะซอลต์ในบริเวณนี้ได้นำเอาหิน  
แปรกล่อมระดับลึกชนิดแกรนูไลต์ที่มีพลอยทับทิมฝังอยู่ภายในขึ้นมาสู่ผิวโลกพร้อมๆกับหิน  
แปรกล่อมอัลตราเมฟิกชนิดเพอร์โดไทต์และไพรอกซิไนต์ ซึ่งหินแปรกล่อมนี้มีองค์ประกอบ  
ทางเคมีเทียบเคียงได้กับหินบะซอลต์ โดยมีเนื้อหินที่แสดงถึงลักษณะการแปรสภาพภายใต้แรง  
กดดันระดับสูงและการเกิดขอบปฏิกิริยาขอบเม็ดแร่ที่ซับซ้อนประกอบร่วมกับลักษณะทางเคมีที่  
ปรากฏที่บ่งชี้ถึงการแปรสภาพระดับแกรนูไลต์ของชั้นหินต้นกำเนิดที่น่าจะเทียบเคียงได้กับชั้นหิน  
อัคนีชนิดเมฟิกที่การสลับชั้นระหว่างหินเนื้อแกรโบกับหินเนื้ออนอร์โทไซต์ ภายใต้ช่วงสมดุล  
ภาวะ ~750-1500°C และ 5-5-23 kb เทียบเท่ากับช่วงความลึกระดับเปลือกโลกชั้นล่าง (~20  
km) ทะลุผ่านช่วงชั้นรอยต่อ Moho (~44 km) ลึกลงไปถึงในชั้นเนื้อโลกส่วนบน (~75 km) ซึ่ง  
คาบเกี่ยวกับช่วงความลึกที่แมกมาบะซอลต์ถือกำเนิด (~30-90 km) โดยมีภูเขาไฟปะทุและนำ  
พลอยจากที่ลึกขึ้นสู่ผิวโลกหลายครั้งในช่วงปลายไพลโอซีน ถึง ไพลสโตซีน (~ 2-0.8 ล้านปีที่ผ่านมา)

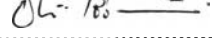
ภาควิชา .....ธรณีวิทยา ..... ลายมือชื่อนิสิต .....   
สาขาวิชา ...ธรณีวิทยา ... ลายมือชื่อ อ.ที่ปริกษานิพนธ์หลัก .....   
ปีการศึกษา.... 2553..... ลายมือชื่อ อ.ที่ปริกษานิพนธ์ร่วม ..... 

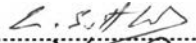
## 4973821923 : MAJOR GEOLOGY

KEYWORDS: RUBY/ XENOLITH / GRANULITE / BASALT / GENESIS /  
THERMOBAROMETRY / DATING / KENYA

TAWATCHAI CHUALAOWANICH: PETROGENESIS OF RUBY-BEARING  
XENOLITH FROM SIMBA AND EMALI BASALTIC TERRANES, KENYA.  
ADVISOR: ASST.PROF. CHAKKAPHAN SUTTHIRAT, Ph.D., CO-ADVISOR:  
ASSOC.PROF. VISUT PISUTTHA-ARNOND, Ph.D.,

Abundant ruby-bearing granulite xenoliths have been found in association with ultramafic xenoliths in the northern Chyulu Volcanic Province, within two small basaltic terranes of the Nguu Hills and the Ngulai Hills, located in the vicinity of Simba town, SE Kenya. The host basalts belong to an alkali affinity ranging in chemical composition from foidite to tephite/basanite. These chemical characteristics suggest that the magmas have been derived from partial melting of an amphibole- and/or phlogopite-bearing spinel lherzolite in the upper mantle source region that involves the interaction between pre-existing zones of lithospheric weak zones, caused by the evolution of the Mozambic Belt (~500-800 Ma), and slightly upwelling of mantle plume. The observed xenoliths, e.g. peridotite, pyroxenite and granulite, bear equivalent basaltic composition. However, complex reactions, as well as plastic deformation, combined with geochemical characteristics of these xenoliths may lead to progressive transformation of a layering mafic (gabbroic/anorthositic) cumulate protolith including corundum-bearing formation and other related rocks under a condition of granulite facies. Based on geothermobarometric constraints, these rocks appear to have undertaken high P-T ranges of ~750-1500°C and 5-23 kb equivalent to depths of the lower crust (~20 km) across the Moho (~44 km) down to the upper mantle (~75 km), corresponding to where the host magmas generated (~30-90 km). The corundum-related basalt eruptions had intermittently occurred during late Pliocene (2.1±0.09 Ma) to middle Pleistocene (0.83±0.03Ma) times.

Department : ..... Geology ..... Student's Signature : 

Field of Study : ..... Geology ..... Advisor's Signature : 

Academic Year : ..... 2010 ..... Co-Advisor's Signature : 

## ACKNOWLEDGEMENTS

This study is financially supported by (1) the Gem and Jewelry Institute of Thailand (Public Organization) for fieldwork expenses and (2) the 90<sup>th</sup> Anniversary of Chulalongkorn University Fund (Ratchadaphiseksomphot Endowment Fund) for laboratorial and other research expenses. Profound acknowledgement goes to my advisor, Assistant Professor Dr. Chakkaphan Sutthirat, Department of Geology Department, Faculty of Science, Chulalongkorn University for his valuable supervision, encouragement and patient. I acknowledge to my co-advisor, Associate Professor Dr. Visut Pisuttha-arnond and other thesis committee for their kind support and understanding.

I felt in debt to Mr. and Mrs. Kennedy for allowing us to access their prospecting area, providing transportation support in field and lending Mr. Muia Boneface Mutunai to be my great assistant throughout the course of fieldwork. Additionally, I am thankful to my dear friend, Mr. Suvapak Imsamut, a senior geologist from the Department of Mineral Resources of Thailand (DMR) for helping me get through the fieldwork with ease.

I would like to extend my deep appreciation to persons from following institutes; (1) *DMR*: Ms. Suchada Sripairojthikoon, Ms. Benjamas Kongaphirak and their crews from for providing XRF and FeO analyses and Mr. Chalermwong and Mr. Pissanu for help preparing thin section and polished thin sections, (2) *Department of Geoscience, National Taiwan University*: Professor Dr. Ching-Hua Lo and his assistant Mr. Sue for Ar-Ar dating and Professor Dr. Sun-Lin Chung and Ms. I-Jhen Lin for ICP-MS assistance, (3) *Department of Earth Sciences, National Taiwan Normal University*: Professor Dr. Tung-Yi Lee and Assistant Professor Dr. Mong-Wan Ye as well as their graduate students for kind hospitality, and (4) *Department of Geology, Chulalongkorn University*: Ms. Sopit Poompuang for helping with EPMA procedure. Without them, my laboratorial tasks could not be accomplished.

There are still many persons who have both directly and indirectly contributed to my research study but unnamed. I, therefore, would like to finalize my express of gratification to those I have omitted afore.

## CONTENTS

	Page
ABSTRACT (THAI) .....	iv
ABSTRACT (ENGLISH).....	v
ACKNOWLEDGEMENTS.....	vi
CONTENTS.....	vii
LIST OF TABLES.....	ix
LIST OF FIGURES.....	x
CHAPTER I INTRODUCTION.....	1
1.1 General Statement.....	1
1.2 Objectives and Aims.....	3
1.3 Geological Setting.....	3
1.4 Methodology.....	8
1.5 Organization of Thesis Report.....	12
CHAPTER II BASALTS.....	14
2.1 Introduction.....	14
2.2 Petrographic Descriptions.....	14
2.2.1 Nguu Hills Basalts .....	15
2.2.2 Ngulai Hills Basalts.....	17
2.2.3 Chyulu Basalts.....	17
2.3 Geochemical Characteristics.....	20
2.3.1 Rock Discrimination.....	20
2.3.2 Whole-rock Geochemistry .....	27
2.4 Geochronology of Basalts.....	33
CHAPTER III XENOLITHS.....	39
3.1 Introduction.....	39
3.2 Petrographic Descriptions .....	40
3.2.1 Group 1: Peridotites.....	40
3.2.2 Group 2: Pyroxinites.....	44
3.2.3 Group 3: Granulites.....	47
3.3 Geochemistry of Xenoliths.....	50
3.4 Mineral Chemistry of Xenoliths.....	62
3.4.1 Olivine.....	62

3.4.2 Orthopyroxene.....	64
3.4.3 Clinopyroxene.....	68
CHAPTER IV GEOTHERMOBAROMETRY.....	71
4.1 Introduction.....	71
4.2 Geothermobarometry of Basalts.....	72
4.3 Geothermobarometry of Xenolith.....	81
CHAPTER V DISCUSSION AND RECOMMENDATIONS.....	90
REFERENCES.....	106
APPENDICES.....	119
Appendix A: X-ray Mapping Images.....	120
Appendix B: Criteria for Accepting/Rejecting EPMA Analyses.....	126
BIBIOGRAPHY.....	129



## LIST OF TABLES

		Page
Table 2.1	Whole-rock analyses of major oxides and CIPW norm of basalts from the Nguu Hills lavas. ....	22
Table 2.2	Whole-rock analyses of major oxides and CIPW norm of basalts from the Ngulai Hills and Chyulu (Kiboko) lavas. ....	23
Table 2.3	Whole-rock analyses of selected trace elements of basalts from the Nguu Hills lavas. ....	24
Table 2.4	Whole-rock analyses of selected trace elements of basalts from the Ngulai Hills and Chyulu (Kiboko) lavas. ....	25
Table 2.5	Ranges of major and selected trace elements of the studied basalt samples .....	26
Table 2.6	$^{40}\text{Ar}/^{39}\text{Ar}$ analytical data for dated specimens. Rows with bold italic numeric represent a set of heating step selected for plateau age estimation. ....	34
Table 3.1	Type of xenoliths from the studied locales. Numbers begun with Ng are from Nguu Hills specimens and the less from Ngulai Hills. New forming mineral phases are in brackets.....	41
Table 3.2.	Whole-rock major oxide analyses and CIPW normative mineralogy of representative samples of each specimen group of xenoliths, analyzed by WD-XRF. ....	51
Table 3.3	Whole-rock trace element analyses of representative samples of each specimen group of xenoliths, analyzed by ICP-MS. ....	53
Table 3.4	Representative EPMA of olivine. ....	63
Table 3.5	Representative EPMA of orthopyroxene.....	65
Table 3.6	Representative EPMA of clinopyroxine.....	69
Table 4.1	Temperatures and pressures estimated using the clinopyroxene-basalt thermobarometer of Putirka <i>et al.</i> (1996). ....	75
Table 4.2	Temperatures and pressures estimated using the clinopyroxene-basalt thermobarometer of Putirka <i>et al.</i> (2003). ....	76
Table 4.3	Average temperatures at given pressures (Pest) estimated using the olivine-basalt thermometer of Putirka <i>et al.</i> (2007). ....	79
Table 4.4	Summarized ranges of P-T constraint of each representative xenoliths from the Nguu and Ngulai Hills derived from a line intersection between a thermometer and barometer pair. ...	81

## LIST OF FIGURES

		Page
Figure 1.1	Ruby exploration area, licensed to Gemstone International Mining Ltd., at Nguu Hills. A) Topography of the area covered by basaltic flow. B-D) Prospecting activities, with primitive tools, took place along steam branches. E) Color shades of ruby and purple sapphire from the area. F) Left over gravels comprising basalt, xenoliths and basement fragments.	2
Figure 1.2	Satellite image displaying topographic features around the study area in the proximity of Simba town, SE Kenya. Dashed circles represent the areas where xenoliths were collected. (Image source: downloaded from Google Earth).	4
Figure 1.3	Simplified geological map showing the distribution of the Cenozoic volcanic units of the northernmost part of the Chyulu Hills volcanic field outcropping in the vicinity of Simba town (modified after Saggerson, 1963). Rectangle blocks mark the studied areas (1) Nguu Hills and (2) Ngulai Hills volcanic subterranean.	5
Figure 1.4	Schematic diagram showing methodology framework of this study.	9
Figure 2.1	Photomicrographs of basalt samples from the Nguu Hills area showing: microporphyritic textures with various sizes of phenocrysts and groundmass, stage of iddingsite (id) replacement and vesicular contents. (a) Finest matrix with low id substitution. (b) coarser matrix with moderate id substitution. (c) Most part of matrix replaced by id. (d) Size difference among olivine (ol) phenocrysts and a spinel (spl)-ol composite xenocryst. (e) Plagioclase (pl) and clinopyroxene (cpx) xenocrysts. (f) Rare cpx xenocryst with symplectic rind and abundant titanomagnetite (Ti-mt) in groundmass..	16
Figure 2.2	Microscopic views of basalts from the Ngulai Hills area showing microporphyritic textures with variation in sizes of phenocrysts and groundmass and vesicular contents. <i>Left:</i> (a) Sub-idiomorphic olivine (ol) and clinopyroxene (cpx) phenocrysts in finest matrix from Kwa Mbiti. (b) Quartz xenocryst in coarser microlite matrix from Kyanduini. (c) Microporphyric in fine seriate matrix from Kwa Nthuku. <i>Right:</i> (d) Sub-idomorphous cpx, ol and plagioclase (pl) phenocrysts in finest matrix from Kwa Nthugu resembling to that from Kwa Mbiti. (e) Titanomagnetite (Ti-mt) and spinel (spl) intergrowth with cpx from Kwa Nthuku. (f) Basalt with moderate iddingsite (id) replacement from Ol Doinyo Orkaria.	18

Figure 2.3	Microscopic views of basalts from the Chyulu basalts showing microporphyritic textures containing olivine (ol) and clinopyroxene (cpx) and magnetite (mt) phenocrysts in fine-grained groundmass. <i>Left: (a)</i> Sub-idiomorphic phenocrysts with partial alignment of microlite matrix from Mwailo cone. <i>(b)</i> Cluster of cpx phenocrysts in coarser microlite matrix from basaltic flow near Hunter's Lodge, Kiboko. <i>Right: (c)</i> Compositional zoning in cpx phenocryst from basaltic flow near Omaki cone. <i>(d)</i> Crossed-polar image of B.	19
Figure 2.4	Classification diagrams for the basalts of the Nguu and Ngulai basaltic fields <i>(a)</i> after LeBas <i>et al.</i> , (1986), <i>(b)</i> after Cox <i>et al.</i> , (1979). The dividing line between alkali and sub-alkalic lava series is after Miyashiro (1978), and <i>(c)</i> after De La Roche <i>et al.</i> (1980).	27
Figure 2.5	Plots of wt. % major oxides versus wt. % MgO for basaltic rocks from the Nguu Huills, Ngulai Hils, and some of the recent Chyulu lavas. All oxides were notmalized to 100 % on a volatile-free basis before plotting.	28
Figure 2.6	Plots of trace element (ppm) and CaO/Al <sub>2</sub> O <sub>3</sub> versus MgO (wt. %) and Al <sub>2</sub> O <sub>3</sub> versus CaO/Al <sub>2</sub> O <sub>3</sub> for basaltic rocks from the Nguu Huills, Ngulai Hils, and some of the recent Chyulu lavas.	29
Figure 2.7	Plots of Nb, Rb, Ce and La versus Zr for basaltic rocks from the Nguu Huills, Ngulai Hils, and some of the recent Chyulu lavas.	30
Figure 2.8	Mantle-normalized trace element variation diagrams for basaltic rocks from the Nguu Huills, Ngulai Hils, and some of the recent Chyulu lavas.	32
Figure 2.9	Chondrite-normalized REE paterns for basaltic rocks from the Nguu Huills, Ngulai Hils, and some of the recent Chyulu lavas.	36
Figure 2.10	Plots showing apparent age fraction of <sup>39</sup> Ar released at each heating step for selected basaltic specimens from the Nguu and the Ngulai Hils.	37
Figure 2.11	Plots showing apparent age fraction of <sup>39</sup> Ar released at each the Chyulu lavas.	38
Figure 2.12	Plots showing plateau age of the dated specimen along the fractionation trends of the basalts from the study area.	
Figure 3.1	Modal abundances of peridotite and pyroxenite xenoliths from the studied locales. Filled square represents corudum-bearing variety.	42

**Figure 3.2** Group 1 xenoliths selected for petrographic study: A. spl wehrlite (Ng18: left) and grt-spl lherzolite (Ng07: right). B. (Ng07) Opx is in mutual contact with ol and cpx (Ng07). C. (Ng 18) Mottled clinopyroxenes (cpx), with spongy texture and kelyphite rims, are in mutual contact with unaltered olivine (ol). D. (Ng07) Thin reaction zone containing small laths of plagioclase rimming around spinel (spl). E. (Ng18) Back-scattered electron image (BSE) reveal fine exsolution lamella and mottled texture in cpx as well as reaction rind around spl. F. (Ng07) BSE image show spongy texture on a part of cpx and spl encrusted by patches of kelyphite taking spaces between ol and cpx.

43

**Figure 3.3** Group 2 pyroxenite xenoliths selected for petrographic study: A. medium-grained websterite (Ng22: right ) and fine-grained spinel websterite (Ng27: left). B. (Ng12) Granoblastic texture of opx and cpx with exsolution lamella and rimmed by thin kelyphitic garnet network. C. (Ng22) Opx is overgrown by 2nd clinopyroxene (cpxII). D. (Ng 23) kelyphite (kely) corona cored with corundum (crn) and green spinel (spl). Crn in contact with spl is observed in crn-bearing websterite. E. (Ng12) Back-scattered electron image (BSE) of the websterite shows with kelyphite filled in along bended cleavages of opx. Small quartz grains occur within reaction band rimming opx. F. (Ng33) BSE image of the orthopyroxenite shows kalyphitic corona around opx and this opx partly turned to cpx. Map showing the distribution of faults in eastern Myanmar including western and northwestern Thailand regions (Natalaya et al., 1985).

45

**Figure 3.4** (Left) Major varieties of rough specimens of group 3 mafic granulite xenoliths: A. sharp banded corundum (crn)-bearing (Ng27), C. foliated crn-bearing (OK02), and E. non-foliated, polygonal crn-barren (KMb01). (Right) Photo images: B. (Kka04) showing cluster of polygonal kelyphite (kely) with garnet (grt) cored in contact with clinopyroxene (cpx), corundum (crn) and recrystallized plagioclase (pl). Thin corona of quartz (qtz) wrapping cpx is expressed. D. (KNt02) Back-scattered electron image (BSE) displays crn in direct contacts with spl and rutile (Rt). F. (KMb01) BSE image shows orthopyroxene (opx), with strings of qtz intergrowth, mantled by cpxII and kely coronas

48

	Page	
Figure 3.5	a) LeBas <i>et al.</i> classification diagrams for xenoliths from the study sites around the Nguu Hills and Ngulai Hills in comparison to their basaltic hosts. b) The alkaline/sub-alkaline subdivision diagram according to De LeRoche <i>et al.</i> (1980).	55
Figure 3.6	MgO variation diagrams for selected major oxides in the studied xenoliths	56
Figure 3.7	MgO variation diagrams for selected trace elements in the studied xenoliths	57
Figure 3.8	Pyroxene mantle normalized patterns of the studied xenoliths compared with representative basalts. Normalization values are from McDonough and Sun (1995).	60
Figure 3.9	Chondrite normalized REE patterns of the studied xenoliths. Normalization values are from Sun and McDonough (1989)	61
Figure 3.10	Pyroxene plots of Fe <sup>2+</sup> -Ca-Mg atomic proportions of orthopyroxenes and clinopyroxenes in peridotite, pyroxenite and granulite xenoliths.	67
Figure 4.1	P-T diagrams of the studied basalt specimens estimated using clinopyroxene-liquid thermobarometers of Putirka <i>et al.</i> (1996: top) and (2003: bottom)	77
Figure 4.2	Average temperature of each studied basalt specimen estimated using olivine-liquid thermometer of Putirka <i>et al.</i> (2007). Blue bar inside the legend box represents approximate SD of T calculation	80
Figure 4.3	a) P-T constraints of spinel lherzolite, Ng07, according to 5 different thermo-barometers including (1) Cpx-Opx (Brey and Köhler, 1990), (2) Ol-Spl (Ballhaus <i>et al.</i> , 1991), (3) Ol-Cpx (Ai, 1994) and (4) Grt-Spl (Perchuk, 1991) thermometers, and (5) Grt-Opx thermobarometer (Aranovich and Berman, 1997). Star symbol marking the best-fit P-T condition within the constraint area. b) P-T constraints of spinel wehrlite, Ng18, according to 4 different thermo-barometers including (1) Cpx-Opx (Brey and Köhler, 1990), (2) Ol-Spl (Ballhaus <i>et al.</i> , 1991) and (3) Ol-Cpx (Ai, 1994) thermometers, and (4) Grt-Opx thermobarometer (Aranovich and Berman, 1997). Star symbol marking the best-fit P-T condition within the constraint area.	83
Figure 4.4	P-T constraints of spinel-free websterite, Ng34, according to 2 different thermo-barometers including (1) Cpx-Opx thermometer (Brey and Köhler, 1990) and (2) Grt-Opx thermobarometer (Aranovich and Berman, 1997). Star symbol marking the best-fit P-T condition within the constraint area.	84

- Figure 4.5. a) P-T constraints of foliated mafic granulite, *KNt01*, according to 5 different thermobarometers including (1) Cpx-Opx (Brey and Köhler, 1990), (2) Grt-Cpx (Ai, 1994) and (3) Grt-Opx (Aranovich and Berman, 1997) thermometers, and (4) Grt-Cpx-Pl-Qtz (Eckert *et al.*, 1991) and (5) Grt-Opx-Pl-Qtz (Lal, 1993) barometers. Star symbol marking the best-fit P-T condition within the constraint area. b) P-T constraints of banded mafic granulite, *Ng21*, according to 4 different thermobarometers including (1) Cpx-Opx (Brey and Köhler, 1990) and (2) Grt-Opx (Aranovich and Berman, 1997) thermometers, and (3) Grt-Cpx-Pl-Qtz (Eckert *et al.*, 1991) and (4) Grt-Opx-Pl-Qtz (Lal, 1993) barometers. Star symbol marking the best-fit P-T condition within the constraint area.. 85
- Figure 4.6 P-T constraints of felsic granulite, *KMb01*, according to 4 different thermo-barometers including (1) Cpx-Opx (Brey and Köhler, 1990) and (2) Grt-Opx (Aranovich and Berman, 1997) thermometers, and (3) Grt-Cpx-Pl-Qtz (Eckert *et al.*, 1991) and (4) Grt-Opx-Pl-Qtz (Lal, 1993) barometers. Star symbol marking the best-fit P-T condition within the constraint area. 86
- Figure 4.7 Pseudosection diagrams of the peridotite xenoliths represented by Spl lherzolite (*Ng07*: left) and the Spl wehrlite (*Ng18*: right). 88
- Figure 4.8 Pseudosection diagrams of the pyroxenite xenoliths represented by Spl-free websterite (*Ng34*: left) compared to the pyroxene-rich band of the crn-bearing granulite (*KNt02\_2*: right). 88
- Figure 4.9 Pseudosection diagrams of the granulite xenoliths represented by foliated, Crn-bearing mafic granulite (*Ng21*: left) compared to the crn-barren felsic granulite (*KMb01*: right). 89
- Figure 5.1 Plots of  $K/Th^*$  ( $=K_2O \cdot 10,000/Th$ ) versus Th (ppm) for the basaltic rocks from the Nguu Hills, Ngulai Hills, and Kiboko (Chyulu) lavas in comparison to the published data ranges from the Chyulu Hills and the Western Rift of Rungwe and Muhavura volcanic provinces. Dotted and dashed borders are from Furman (2007). 92

- Figure 5.2 Covariation plot of  $^{143}\text{Nd}/^{144}\text{Nd}$  vs.  $^{87}\text{Sr}/^{86}\text{Sr}$  displaying a broad negative trend from less radiogenic values in northern section of the Eastern Kenya Rift (NRK) towards higher radiogenic compositions observed in the Western Kenya Rift of the Kivu, Rungwe, Karisimbi and Muhavura volcanic regions. The values from the Chyulu Hills are within the lower part of the NKR approaching towards the field of HIMU. Point data for Chyulu Hills and Nguu Hills lavas are from Späth *et al.* (2001). 94
- Figure 5.3 Covariation plot of  $^{208}\text{Pb}/^{204}\text{Pb}$  vs.  $^{206}\text{Pb}/^{204}\text{Pb}$  displaying a broad positive trend for northern Kenya Rift lavas (NKR) and southern Kenya Rift, both off-rift (Chyulu Hills) and within-rift (SKR), towards HIMU. Point data for Chyulu Hills and Nguu Hills lavas are from Späth *et al.* (2001). 95
- Figure 5.4 Showing Chondrite-normalized REE patterns for a) the cogenetic lavas from the Nguu Hills, Ngulai Hills, and Kiboka areas. b) equilibrium batch melts of an amphibole-bearing spinel lherzolite source. c) equilibrium batch melts of an amphibole-garnet-bearing spinel lherzolite source. d) fractional melts of an amphibole-bearing spinel lherzolite source. Normalizing values from Sun and McDonough (1989). 97
- Figure 5.5 P-T constraint diagrams of the xenoliths compared to the host basalts. 98
- Figure 5.6 The Ti-V discrimination diagram for the xenoliths and their host basalts from the Nguu Hills and Ngulai Hills areas. IAT is standed for island arc tholeite and BAB is back arc basin. Lines represent Ti/V ratio. 102
- Figure 5.7 Cartoon summarizing the major features of deep structure underneath the study area and the Chyulu Volcanic Province (modified after Novak *et al.*, 1997). Filled numbered ellipses represent ultramafic layers where 1 is peridotite and 2 is pyroxenite (plagioclase-free websterite). Filled numbered rectangles represent granulite layers where 3.1 is corundum-bearing mafic granulite and 3.2 is corundum-free felsic granulite. Filled triangles are basalt bodies. 103